How to cite: *Angew. Chem. Int. Ed.* **2023,** *62,* e202302032
doi.org/10.1002/anie.202302032

Phthalocyanines

C_{64} Nanographene Tetraimide—A Receptor for Phthalocyanines with Subnanomolar Affinity

*M. A. Niyas, Kazutaka Shoyama, and Frank Würthner**

Abstract: Phthalocyanines are extensively used by the dye and pigment industry and in photovoltaic and photodynamic therapy research due to their intense absorption of visible light, outstanding stability, and versatility. As pigments, the unsubstituted phthalocyanines are insoluble owing to strong intermolecular π-π-stacking interactions, which causes limitations for the solution chemistry for both free base and metalated phthalocyanines. Here we show a supramolecular host–guest strategy to dissolve phthalocyanines into solution. C_{64} nanographene tetraimide (**1**) binds two free base/zinc/copper phthalocyanines in a 1:2 stoichiometry to solubilize phthalocyanines as evidenced by ^{1}H NMR spectroscopy, UV/Vis absorption and single-crystal X-ray analysis. Binding studies using a tetra-*tert*-butyl-substituted soluble phthalocyanine revealed binding affinities of up to $10^9\ M^{-1}$ in tetrachloromethane, relating to a Gibbs free energy of $-52\ kJ\,mol^{-1}$. Energy decomposition analysis revealed that complexes between **1** and phthalocyanines are stabilized by dispersion interactions followed by electrostatics as well as significant charge-transfer interactions.

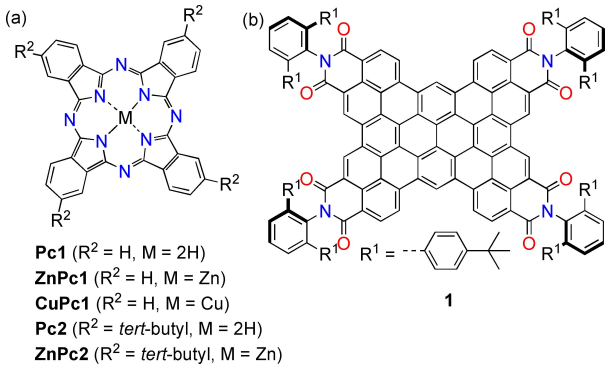

Figure 1. Chemical structures of a) Pc derivatives and b) receptor **1**.Dash in '*tert*-butyl' in Figure 1 is changed from en-dash to hyphen.

Phthalocyanines (Pcs) are an important class of compounds with four isoindole units joined by nitrogen atoms to form an aromatic macrocycle (Figure 1a).[1] Following Linstead's pioneering work, Pcs and metal phthalocyanines (MPc)[2] attracted worldwide interest in scientific and industrial applications.[3] Among those, the utilization of copper Pc as the largest produced organic pigment, utilized in its β-polymorphic state as cyan colorant, stands out. But there are many more applications of this highly stable aromatic and unique 18 π-electron system macrocyclic scaffold owing to its intense absorption of visible light, high stability, and moderate cost of manufacture, i.e. as colorants for printer inks, tattoo inks as well as for textile or paper dyeing, for colour filters in liquid-crystal displays, as colour toners in photocopiers and laser printers, as semiconductors for organic photovoltaics, and as photosensitizers in photodynamic therapy.[3–5] Unsubstituted Pcs (**Pc1** and **MPc1**, Figure 1a) are in general highly crystalline and are insoluble in organic or aqueous solvents. Although peripheral substitutions have been used to study Pcs in solution phase,[6] many large-scale applications still use unsubstituted Pcs.[3,7] For instance, the β-polymorph of **CuPc1** (known as Pigment Blue 15:3) is the only blue pigment in European tattoo industry and is now banned due to concerns over health hazards.[8] Dissolving such insoluble Pcs in their monomeric form in solution is important but challenging due to strong intermolecular interactions between these extended planar π-systems and the resulting thermodynamically very stable non-meltable crystalline state (sublimation temperatures $>500\,°C$).[9] Inspired by reported examples for high affinity synthetic hosts[10] and our earlier work on the binding of polycyclic aromatic hydrocarbons by expanded π-receptors[11,12] we hypothesized that such electron-deficient π-receptors should be able to dissolve also monomeric unsubstituted Pc compounds into solution phase.[10] Here we show that C_{64} nanographene tetraimide **1** can bind unsubstituted Pcs and MPcs and keep them dissolved in organic solvents by supramolecular host–guest interactions. The structural evidence obtained by ^{1}H NMR experiments at slow exchange regime and single crystal X-ray analysis revealed a 1:2 stoichiometric complex formation. Binding studies with soluble tetra-*tert*-butyl substituted Pc (**Pc2**)

[*] M. A. Niyas, Dr. K. Shoyama, Prof. Dr. F. Würthner
Institut für Organische Chemie,
Universität Würzburg
Am Hubland, 97074 Würzburg (Germany)
E-mail: wuerthner@uni-wuerzburg.de
Dr. K. Shoyama, Prof. Dr. F. Würthner
Center for Nanosystems Chemistry (CNC),
Universität Würzburg
Theodor-Boveri-Weg, 97074 Würzburg (Germany)

showed a subnanomolar affinity in apolar organic solvents for a 1:2 stoichiometric complex.

C_{64} nanographene **1** (Figure 1b) was synthesized by a palladium catalysed one-pot cascade annulation reaction between pyrene tetra boronic acid pinacol ester and dibromonaphthalimide.[12] Four terphenyl groups on the imide positions prevent **1** from self-aggregation while allowing aromatic guest molecules of size <**1** to bind on both π-faces. The guest molecule **Pc1** (Figure 1a) has indeed a perfect shape and size complementarity to C_{64} nanographene **1**, ideal for benefiting from dispersion interactions.[13] Further, tetraimide **1** has a low-lying LUMO energy level, which should, similar as demonstrated by Martín and others for so-called electron-rich bucky catchers for the solubilization of C_{60},[14] provide in addition to the common dispersion interactions additional charge-transfer interactions to electron-rich Pcs. Thus, we anticipated that **1** can bind **Pc1** with ultra-strong binding affinities that should enable dissolution of insoluble Pcs into common organic solvents.

To test our hypothesis, we added insoluble **Pc1** into a solution of **1** in $CHCl_3$ and found that the red colour of **1** was changed to dark purple. The colour change indicated that **Pc1** was dissolved due to the presence of **1** (no colour was observed in the absence of **1** in $CHCl_3$). Single crystals were obtained from a defined 1:2 stoichiometry of **1** and **Pc1** by slow vapour diffusion of *n*-hexane into a $CHCl_3$ solution over 3 days. The obtained crystal structure of **1**·2**Pc1** confirmed the 1:2 stoichiometry of host and guest in the noncovalent complex (Figure 2, Table S1).[15] The crystal structure revealed a 1:2 stoichiometric complex that is dimerized to form a hexalayer complex (Figure 2). We then used ^{1}H NMR titration to determine the identity of the noncovalent species formed upon addition of solid **Pc1** to a solution of **1**. Even at 295 K in the rather competitive solvent $CDCl_3$ (known for its excellent solubilization of aromatic π-scaffolds) the ^{1}H NMR titration revealed the stepwise binding of guest to host at the thermodynamic equilibrium. Furthermore, separate signals for host, 1:1 and 1:2 host–guest complexes show that the dynamics of guest exchange are in the slow exchange regime, which is typical for strongly bound supramolecular complexes (Figure 3, Figure S2). Upon addition of 0.5 equiv of **Pc1**, ^{1}H NMR signals of **1** split into monomeric **1** and a set of new signals corresponding to 1:1 complex of **1** and **Pc1**. Evidence of 1:1 stoichiometry comes from the splitting of *tert*-butyl protons of **1** into two new signals. Due to the D_{2h} symmetry of **1**, all the *tert*-butyl protons in the monomeric **1** are chemically equivalent showing only one signal in the ^{1}H NMR spectra. However, as **Pc1** binds, the environment around the protons are different leading to splitting of signals. Owing to the D_{4h} point group of **Pc1**, a 1:1 stoichiometric complex (C_s symmetry) would show two signals while a 1:2 stoichiometric complex (D_{2h} symmetry) shows only one signal for the *tert*-butyl protons of **1** (guest exchange is at slow exchange regime while the guest rotation is at fast exchange). Upon addition of 1.0 equiv of **Pc1**, an additional set of signals emerges with one signal for the *tert*-butyl protons of **1** corresponding to 1:2 complex. At this point, all the three

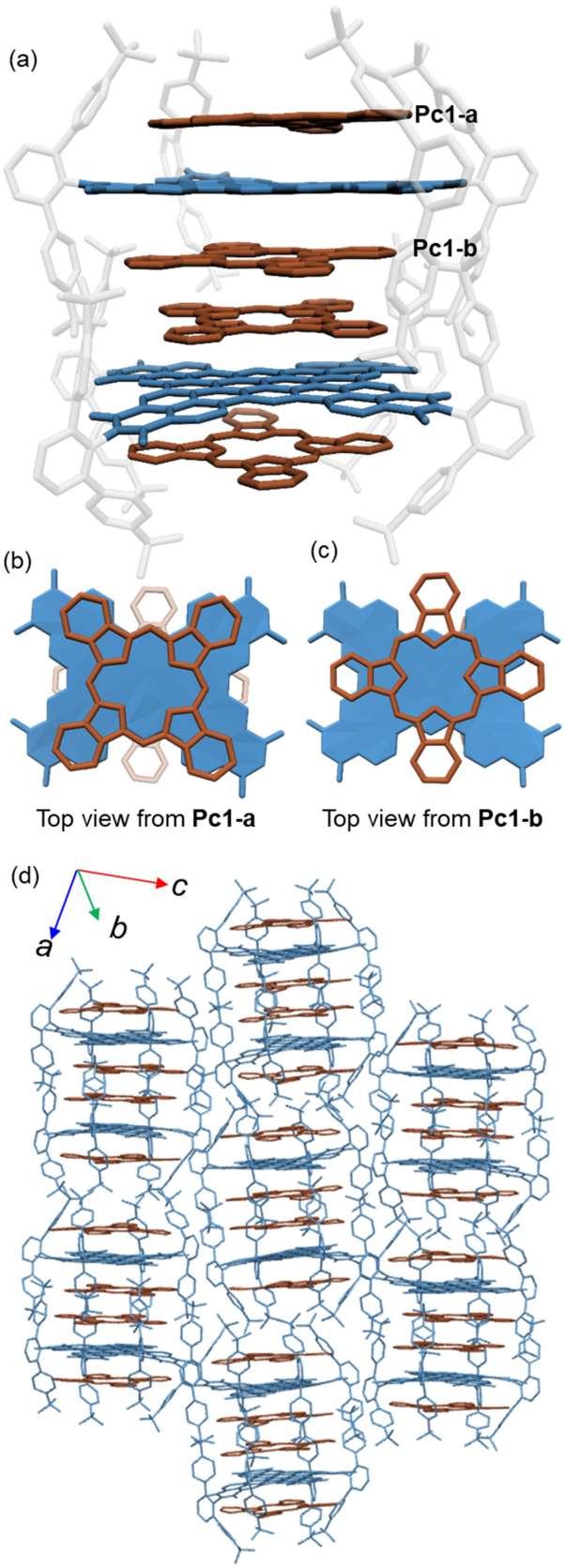

Figure 2. X-ray crystal structure of **1**·2**Pc1** showing a) the hexalayer complex structure, top views from b) **Pc1-a** and c) **Pc1-a**, and d) packing structure.

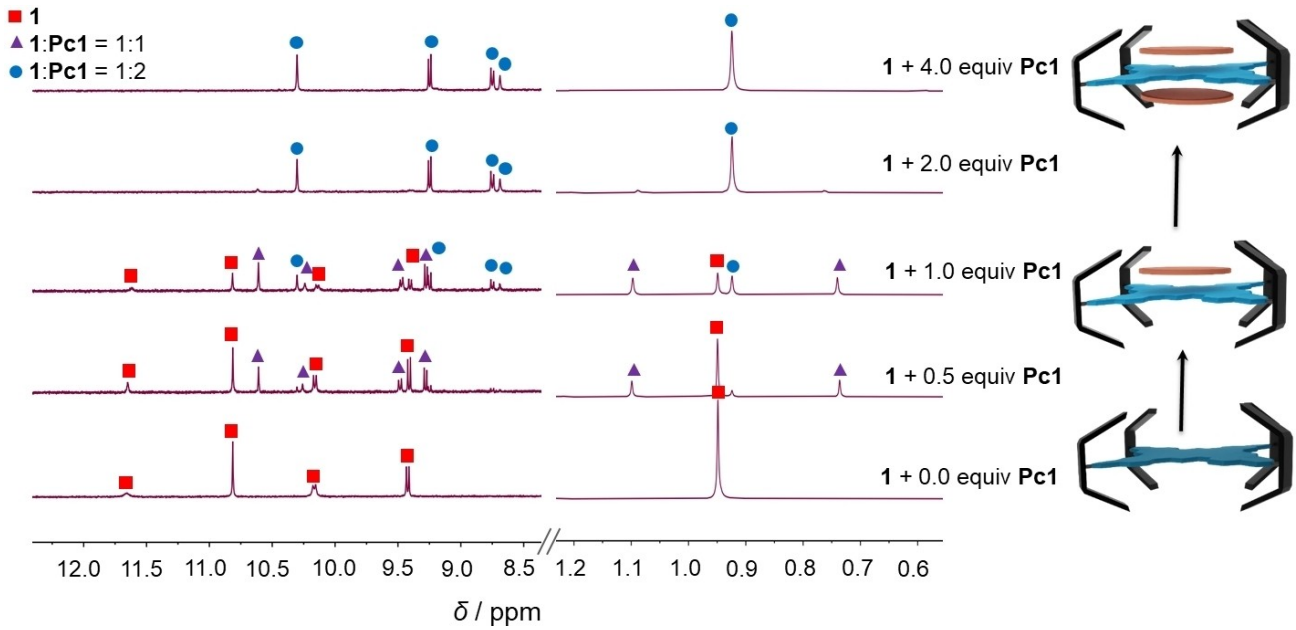

Figure 3. ^{1}H NMR ($CDCl_3$, $c(\mathbf{1}) = 3.6\times10^{-4}$ M, 400 MHz) titration at a slow exchange regime (295 K) showing free host **1**, 1:1 stoichiometric **1**·**Pc1**, and 1:2 stoichiometric **1**·2**Pc1**. Only ^{1}H NMR signals on the aromatic plane of **1** and *tert*-butyl chains of **1** are shown for clarity. Aliphatic protons on the *tert*-butyl substituent of **1** are symmetric in the free host and during titration split into two new signals indicating the symmetry breaking due to 1:1 stoichiometric binding. On further titration, one additional signal emerges while all the free and 1:1 complex signals disappear. Thus, the symmetry is regained in the final titration product, which corresponds to a 1:2 stoichiometric complex. Schematic representation of stepwise complexation of **1** and **Pc1** are also shown for free host to 1:1 to 1:2 stoichiometric host–guest complexes as derived from ^{1}H NMR titration at a slow exchange regime.

species (1:0, 1:1, and 1:2 complexes of **1**:**Pc1**) coexist at equilibrium. Further addition of **Pc1** to 2.0 equiv shows only one set of signals corresponding to the 1:2 complex and even further addition to 4.0 equiv does not change the spectra anymore. The non-changing spectra indicate the end of the titration where all nanographene **1** molecules are complexed. Excess addition of **Pc1** did not show any signals for free **Pc1**, indicating its insolubility. The remaining **Pc1** exists in the solid state. Thus, indeed **1** dissolves **Pc1** into solution in a stoichiometric manner such that the maximum amount of **Pc1** dissolved can be two equivalents of **1**.

In order to measure accurate binding constants and to determine the Gibbs energies for the interaction of **1** with Pcs, we next synthesized a highly soluble 2,9,16,23-tetra-*tert*-butyl-29*H*,31*H*-phthalocyanine (**Pc2**) and its zinc-coordinated counterpart **ZnPc2** (Figure 1a).[16] Guest molecules **Pc2** and **ZnPc2** were synthesized as a regioregular isomer (C_{4h} point group) based on the reported procedures (Scheme S1).[16] Single crystals of **1**·2**Pc2** obtained under similar conditions to **1**·2**Pc1** confirmed the 1:2 stoichiometry (Table S2, Figure S1).[15] Further, we went on to quantify the binding affinity using UV/Vis titration experiments (Table 1).

As **1** has a high extinction coefficient ($\varepsilon = 2.96\times10^5\ M^{-1}cm^{-1}$ at $\lambda = 490$ nm in $CHCl_3$), UV/Vis titration at low concentration ($c(\mathbf{1}) = 1.0\times10^{-6}$ M) was conducted to determine the binding constants (Figures S5–S9). The divalent binding event of **1** and **Pc2** showed subnanomolar binding in $CHCl_3$ with a pronounced anti-cooperativity ($K_1 = 4.6\times10^8\ M^{-1}$, $K_2 = 2.2\times10^7\ M^{-1}$). To get insight into the

Table 1: Association parameters of host **1** with **Pc2** and **ZnPc2** guests in different solvents.

Guest	Solvent	K_1 [M^{-1}][a]	K_2 [M^{-1}][a]	ΔG_1 [kJ mol^{-1}][b]	ΔG_2 [kJ mol^{-1}][b]
Pc2	chloroform[c]	4.6×10^8	2.2×10^7	−48.9	−41.4
	toluene[c]	7.7×10^8	1.4×10^7	−50.2	−40.5
	tetrachloromethane[c]	1.5×10^9	1.1×10^7	−51.8	−39.7
ZnPc2	chloroform[c]	1.5×10^8	7.4×10^6	−46.2	−38.8

[a] Association constants $K_{1/2}$ determined using global-fit-analysis with the program bindfit[17] for a 1:2 binding model at 295 K. [b] Gibbs free energies $\Delta G_{1/2}$ (295 K) calculated from $K_{1/2}$ according to $\Delta G_{1/2}(295\ K) = -RT\ln(K_{1/2})$. [c] UV/Vis titration performed at $c(\mathbf{1}) = 1.0\times10^{-6}$ M at 295 K. All binding constants reported are within 0.5 kJ mol^{-1} of error in Gibbs free energy. Experimental details, errors, and mole fraction plots are given in the Supporting Information.

effect of the solvent further studies were performed in the less polar solvents toluene and CCl_4.[18] The first binding constant increased 1.7 times in toluene ($K_1 = 7.7 \times 10^8\ M^{-1}$) and 3.3 times to nanomolar affinity in CCl_4 ($K_1 = 1.5 \times 10^9\ M^{-1}$) while the second binding affinity was maintained ($K_2 = 1.4 \times 10^7\ M^{-1}$ in toluene and $K_2 = 1.1 \times 10^7\ M^{-1}$ in CCl_4). As a comparison of freebase Pc to ZnPc, we also performed binding studies for **ZnPc2** with **1**. **ZnPc2** also showed similar subnanomolar binding in $CHCl_3$ ($K_1 = 1.5 \times 10^8\ M^{-1}$, $K_2 = 7.4 \times 10^6\ M^{-1}$). Although the binding constant is three times lower for **ZnPc2**, the difference only corresponds to 2.7 kJ mol^{-1} in free energy, indicating the effect of the metal ion on binding is rather weak. Thus, our binding affinity investigations showed that the solubilization of **Pc1** by **1** originates from the ultra-strong binding of **1** towards **Pc1**. Such a high binding strength is unusual for apolar molecules in apolar solvents[10a,19] especially for multiple guest binding.[20]

We then conducted an energy decomposition analysis on the crystal structures of **1**·2**Pc1** and **1**·2**Pc2** to investigate the contributing intermolecular interactions. ALMO-EDA (Absolutely Localized Molecular Orbitals–Energy Decomposition Analysis)[21] was used as the method to gauge the nature of intermolecular interactions (Figure S10, Table S4). ALMO-EDA revealed the importance of dispersion interactions followed by electrostatics as the major contributors towards the stabilization of complex in the crystal structure. However, also charge-transfer interactions play a significant role in the stabilization of this host–guest complex as expected from electron-donating and -accepting nature of its components. This effect of charge-transfer interaction is indeed more appreciable when we compare the binding strength of **1** with hexabenzocoronene[12] (**HBC**, $K_1 = 8.1 \times 10^5\ M^{-1}$, $K_2 = 1.6 \times 10^5\ M^{-1}$ in $CHCl_3$), that has a similarly sized π–surface but a lower lying HOMO level compared to Pcs.[22] A much higher affinity (about three orders of magnitude) for the Pc complexes in comparison to **HBC** could be attributed to the enhanced charge-transfer interaction in **1**·**Pc2** due to the energetically better matching HOMO of Pcs with the LUMO of **1**. The crystal structures also provided insights on the origin of the anti-cooperativity for the binding of the two Pc guests on each side of **1**. Thus, analysis of π–π overlap showed differences for the two bound **Pc1** molecules in the 1:2 complex shown in Figure 2b. **Pc1**-**a** has an overlap of 97 % of its flat aromatic π–surface with **1** while **Pc1**-**b** has only 62 % overlap (Figure S11). These observations indicate that **1** and **Pc1** would generate a stronger binding than those of **1** and **Pc2**.

For the second crystal of **1** with **Pc2**, however, the situation is more complex. Here both molecules **Pc2**-**a** and **Pc2**-**b** show an equal π–π overlap of 69 % with **1** (Figure S11), which is rather unexpected from the negative cooperativity factor ($\alpha = 4\ K_2/K_1$, which was in the range of 0.03–0.19) observed by solution experiments (Table S3). Further investigation by ALMO-EDA analysis of each pair of **1**·**Pc2** complex (separate interaction pairs **1**·**Pc2**-**a** and **1**·**Pc2**-**b** were taken from crystal structure coordinates) revealed that strong repulsive interactions dominate for the complex **1**·**Pc2**-**b**, thus making **1**·**Pc2**-**a** the more stable interaction motif in the complex (Figure S12, Table S5).

In our initial studies, we showed that the free base **Pc1** forms a 1:2 stoichiometric host–guest complex with ultra-high binding affinity that led to **Pc1** solubilization. Now we went on to test if this strategy is also applicable to the more interesting metalated counterparts, **ZnPc1** and **CuPc1**. To our delight, UV/Vis absorption spectroscopy revealed the solubilisation of both **ZnPc1** and **CuPc1** through complexation with **1**. New low energy bands at 700 nm in the mixed solution of **1**·**Pc1**/**1**·**ZnPc1**/**1**·**CuPc1** indicate that **Pc1**/**ZnPc1**/**CuPc1** are dissolved due to the presence of **1** (Figure 4a). On addition of **Pc**/**ZnPc1**/**CuPc1** to **1** in $CHCl_3$, the change in absorption bands at 490 nm is similar to the changes seen in concentration dependent UV/Vis spectra of a fixed-ratio for **1** and **Pc2** (Figure 4b). This change in absorption of **1** on addition of guest molecules shows that the solubilisation of **Pc1**/**ZnPc1**/**CuPc1** is due to host–guest complexation. Such changes in absorption spectra are also manifested in the visual colour change of the solution from red (monomeric **1**) to dark purple (**1**·**Pc1**/**1**·**ZnPc1**/**1**·**CuPc1**) on addition of insoluble Pc guests (Figure 4c). Finally, ^{1}H NMR titration at the slow exchange regime (295 K) also showed the stoichiometric capture of **ZnPc1** to form **1**·2**ZnPc1** in $CHCl_3$ similar to **1**·2**Pc1** (Figure S3). Further, a MALDI-TOF mass spectrometric analysis showed formation of 1:1 stoichiometric **1**·**ZnPc1** and 1:2 stoichiometric **1**·2**ZnPc1** complexes (Figure S4).

In conclusion, we showed that insoluble Pc pigments can be dissolved in monomeric form by strong host–guest interactions. C_{64} nanographene **1** acts as a ditopic receptor that binds two Pc/MPcs with ultra-high binding strength, triggering solubilisation of otherwise insoluble Pc/MPcs in organic solvents. Binding constants determined by titration studies showed subnanomolar affinity for both the first and the second binding events in apolar organic solvents. Such high affinity became possible because of the large π-surface of **1** that can interact with flat Pcs through dispersion, electrostatic, and charge-transfer interactions. In our future research we will apply such complexes to perform reactions of Pcs under benign low-temperature conditions[23] and for studies on light-induced processes as well as applications in organic solar cells. Furthermore, we aim for water-soluble derivatives of **1** for the dissolution of Pc pigments in water which might, for example be useful for photodynamic therapy, removal of tattoos, and a variety of other applications.

Acknowledgements

We thank the Deutsche Forschungsgemeinschaft (DFG, German Research Foundation) for financial support (grant no. WU 317/20-2). We acknowledge DESY (Hamburg, Germany), a member of the Helmholtz Association HGF, for providing synchrotron experimental facilities at PETRA III under P11 proposal no. I-20211168. We thank Dr. Eva Crosas for assistance in using beamline P11, Dr. Magnus Mahl for his initial studies on Pc complexation by **1** and

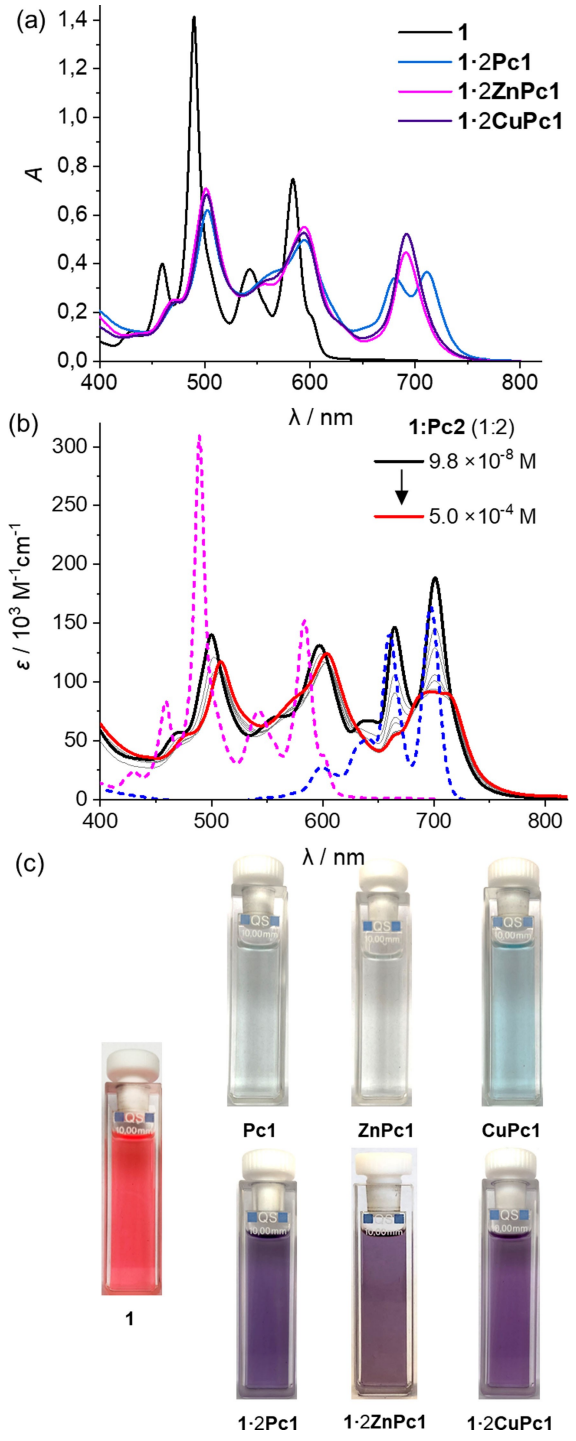

Figure 4. a) UV/Vis absorption spectra of **1** with **Pc1**, **ZnPc1**, and **CuPc1** showing the solubilisation of **Pc1**/**MPc1** due to complexation ($CHCl_3$, c(**1**) = 5.0×10^{-6} M, c(**Pc1/ZnPc1/CuPc1**) = 1.0×10^{-5} M). b) Concentration dependent UV/Vis absorption spectra of a 1 : 2 stoichiometric mixture of **1** and **Pc2** at different concentrations in $CHCl_3$ at 295 K. The dotted spectrum in pink denotes **1** while the dotted spectrum in blue corresponds to **Pc2** in $CHCl_3$ at 298 K. c) Photographs of solutions of host **1** (red colour, c(**1**) = 5.0×10^{-6} M), guests **Pc1**, **ZnPc1**, and **CuPc1** (almost colourless due to very low solubility, c(**Pc1/ZnPc1/CuPc1**) = 1.0×10^{-5} M), and complexes **1**·2**Pc1**, **1**·2**ZnPc1** and **1**·2**CuPc1** (dark purple, c(**1**) = 5.0×10^{-6} M, c(**Pc1/ZnPc1/CuPc1**) = 1.0×10^{-5} M) in $CHCl_3$. The colour change from red to dark purple on addition of guests indicates complexation by the solubilization of guests.Updated figuresComplex names in Figure 4a and 4c are changed from **1**·**Pc1**, **1**·**ZnPc1** and **1**·**CuPc1** to **1**·2**Pc1**, **1**·2**ZnPc1** and **1**·2**CuPc1**.

Julius Albert for technical assistance in synthesis. Open Access funding enabled and organized by Projekt DEAL.

Conflict of Interest

The authors declare no conflict of interest.

Data Availability Statement

The data that support the findings of this study are available from the corresponding author upon reasonable request.

Keywords: Dyes/Pigments · Host–Guest Systems · Nanographenes · Phthalocyanines · Supramolecular Chemistry

[1] *Phthalocyanines—Properties and Applications, Vol. 1–4* (Eds.: C. C. Leznoff, A. B. P. Lever), VCH, New York, **1989**.
[2] a) R. P. Linstead, *J. Chem. Soc.* **1934**, 1016–1017; b) G. T. Byrne, R. P. Linstead, A. R. Lowe, *J. Chem. Soc.* **1934**, 1017–1022; c) R. P. Linstead, A. R. Lowe, *J. Chem. Soc.* **1934**, 1022–1027.
[3] a) P. Erk, H. Hengelsberg, M. F. Haddow, R. van Gelder, *CrystEngComm* **2004**, *6*, 475–483; b) P. Gregory, *J. Porphyrins Phthalocyanines* **2000**, *4*, 432–437; c) P.-C. Lo, M. S. Rodríguez-Morgade, R. K. Pandey, D. K. P. Ng, T. Torres, F. Dumoulin, *Chem. Soc. Rev.* **2020**, *49*, 1041–1056; d) J. Karges, *Angew. Chem. Int. Ed.* **2022**, *61*, e202112236.
[4] E. M. Bauer, T. D. Caro, P. Tagliatesta, M. Carbone, *Dyes Pigm.* **2019**, *167*, 225–235.
[5] a) P. Gregory, *J. Porphyrins Phthalocyanines* **1999**, *3*, 468–476; b) G. de la Torre, C. G. Claessens, T. Torres, *Chem. Commun.* **2007**, 2000–2015; c) C. G. Claessens, U. Hahn, T. Torres, *Chem. Rec.* **2008**, *8*, 75–97.
[6] a) R. D. George, A. W. Snow, J. S. Shirk, W. R. Barger, *J. Porphyrins Phthalocyanines* **1998**, *2*, 1–7; b) M. J. Cook, A. J. Dunn, S. D. Howe, A. J. Thomson, K. J. Harrison, *J. Chem. Soc. Perkin Trans. 1* **1988**, 2453–2458; c) M. J. Cook, *J. Mater. Sci. Mater. Electron.* **1994**, *5*, 117–128.
[7] T. Inabe, H. Tajima, *Chem. Rev.* **2004**, *104*, 5503–5534.
[8] Bundesinstitut für Risikobewertung, *BfR-Stellungnahmen.* **2020**, *2020*, 6, https://doi.org/10.17590/20201006-102053.
[9] A. W. Snow in *The Porphyrin Handbook, Vol. 17* (Eds.: K. M. Kadish, K. M. Smith, R. Guillard), Academic Press, San Diego, **2003**, pp. 129–176.
[10] a) S. Sarkar, P. Ballester, M. Spektor, E. A. Kataev, *Angew. Chem. Int. Ed.* **2023**, *62*, e202214705; b) F. Biedermann, H. J. Schneider, *Chem. Rev.* **2016**, *116*, 5216–5300; c) M. Yoshizawa, L. Catti, *Acc. Chem. Res.* **2019**, *52*, 2392–2404.
[11] B. Teichmann, A.-M. Krause, M.-J. Lin, F. Würthner, *Angew. Chem. Int. Ed.* **2022**, *61*, e202117625.
[12] M. Mahl, M. A. Niyas, K. Shoyama, F. Würthner, *Nat. Chem.* **2022**, *14*, 457–462.
[13] Y. Mao, M. Loipersberger, P. R. Horn, A. Das, O. Demerdash, D. S. Levine, S. Prasad Veccham, T. Head-Gordon, M. Head-Gordon, *Annu. Rev. Phys. Chem.* **2021**, *72*, 641–666.
[14] E. M. Pérez, N. Martín, *Chem. Soc. Rev.* **2008**, *37*, 1512–1519.
[15] Deposition Numbers 2237579 (for **1**·2(**Pc1**)) and 2237578 (for **1**·2(**Pc2**)) contain the supplementary crystallographic data for this paper. These data are provided free of charge by the joint Cambridge Crystallographic Data Centre and Fachinformationszentrum Karlsruhe Access Structures service.

[16] a) N. Iida, K. Tanaka, E. Tokunaga, H. Takahashi, N. Shibata, *ChemistryOpen* **2015**, *4*, 102–106; b) J. Alzeer, P. J. C. Roth, N. W. Luedtke, *Chem. Commun.* **2009**, 1970–1971.
[17] a) D. B. Hibbert, P. Thordarson, *Chem. Commun.* **2016**, *52*, 12792–12805; b) http://supramolecular.org.
[18] F. Würthner, *J. Org. Chem.* **2022**, *87*, 1602–1615.
[19] a) K. N. Houk, A. G. Leach, S. P. Kim, X. Zhang, *Angew. Chem. Int. Ed.* **2003**, *42*, 4872–4897; b) D. B. Smithrud, F. Diederich, *J. Am. Chem. Soc.* **1990**, *112*, 339–343.
[20] a) J. Rebek, *Angew. Chem. Int. Ed.* **2005**, *44*, 2068–2078; b) F. J. Rizzuto, L. K. S. von Krbek, J. R. Nitschke, *Nat. Chem. Rev.* **2019**, *3*, 204–222.
[21] P. R. Horn, Y. Mao, M. Head-Gordon, *Phys. Chem. Chem. Phys.* **2016**, *18*, 23067–23079.
[22] R. Rathore, C. L. Burns, *J. Org. Chem.* **2003**, *68*, 4071–4074.
[23] H. C. Kolb, M. G. Finn, K. B. Sharpless, *Angew. Chem. Int. Ed.* **2001**, *40*, 2004–2021.

Manuscript received: February 9, 2023
Accepted manuscript online: March 15, 2023
Version of record online: May 9, 2023